

Matter power spectrum and the challenge of percent accuracy

Aurel Schneider^{1*}, Romain Teyssier¹, Doug Potter¹, Joachim Stadel¹,
Julian Onions², Darren S. Reed¹, Robert E. Smith³, Volker Springel^{4,5},
and Frazer R. Pearce²

¹*Institute for Computational Science, University of Zurich, 8057 Zurich, Switzerland*

²*School of Physics and Astronomy, University of Nottingham, Nottingham NG7 2RD, United Kingdom*

³*Department of Physics and Astronomy, University of Sussex, Brighton, BN1 9QH, United Kingdom*

⁴*Heidelberger Institut für Theoretische Studien, 69118 Heidelberg, Germany*

⁵*Zentrum für Astronomie der Universität Heidelberg, ARI, 69120 Heidelberg, Germany*

28 May 2022

ABSTRACT

Future galaxy surveys require one percent precision in the theoretical knowledge of the power spectrum over a large range including very nonlinear scales. While this level of accuracy is easily obtained in the linear regime with perturbation theory, it represents a serious challenge for small scales where numerical simulations are required. In this paper we quantify the accuracy of present-day N -body methods, identifying main potential error sources from the set-up of initial conditions to the measurement of the final power spectrum. We directly compare three widely used N -body codes, `Ramses`, `Pkdgrav3`, and `Gadget3` which represent three main discretisation techniques: the particle-mesh method, the tree method, and a hybrid combination of the two. For standard run parameters, the codes agree to within one percent at $k \leq 1 \ h\text{Mpc}^{-1}$ and to within three percent at $k \leq 10 \ h\text{Mpc}^{-1}$. In a second step, we quantify potential errors due to initial conditions, box size, and resolution using an extended suite of simulations performed with our fastest code `Pkdgrav3`. We demonstrate that the simulation box size should not be smaller than $L = 0.5 \ h^{-1}\text{Gpc}$ to avoid nonlinear finite-volume effects. Furthermore, a maximum particle mass of $M_p = 10^9 \ h^{-1}M_\odot$ is required to conservatively obtain one percent precision of the matter power spectrum. As a consequence, numerical simulations covering large survey volumes of upcoming missions such as `DES`, `LSST`, and `Euclid` will need more than a trillion particles to reproduce clustering properties at the targeted accuracy.

Key words: cosmology: theory, methods: numerical

1 INTRODUCTION

In the last decades, cosmology has entered the high precision regime owing to ever more accurate measurements of the Cosmic Microwave Background (CMB). The statistical information of the CMB sky is, however, intrinsically limited, while large scale structures contain a great wealth of modes which can be exploited, provided nonlinear structure formation is well understood. Next-generation galaxy and weak lensing surveys such as `DES`¹, `LSST`², and `Euclid`³ re-

quire percent accurate modelling of the matter power spectrum up to wave numbers of $k \sim 10 \ h\text{Mpc}^{-1}$ in order to fully exploit their constraining power for cosmology (Ivezic et al. 2008; ?).

Standard perturbation theory gives accurate results up to $k \sim 0.1 \ h\text{Mpc}^{-1}$, while numerical simulations are indispensable at higher wave numbers (Carlson et al. 2009; Fosalba et al. 2015). Pure dark matter simulations based on N -body techniques are believed to be accurate up to about $k \sim 1 \ h\text{Mpc}^{-1}$, beyond which baryonic feedback from active galactic nuclei (AGN) must be included (van Daalen et al. 2011).

In this paper we focus on the matter power spectrum from collisionless N -body simulations, ignoring all hydrody-

* Email: aurel@physik.uzh.ch

¹ www.darkenergysurvey.org

² www.lsst.org/lsst

³ sci.esa.int/euclid

namical effects. Although strictly not valid at small scales, this approach is currently the only option for precision cosmology as the relevant AGN feedback mechanism is not well understood, and is poorly constrained by observations. A potential way forward is to study AGN feedback with high resolution simulations of small cosmological volumes and to parametrise the effects on the matter power spectrum. Cosmological parameter estimation can then be carried out on the basis of N -body simulations plus additional free model parameters accounting for the AGN contribution (Mohammed et al. 2014).

Comparison studies of N -body codes and subsequent analysis tools have been performed in the past. The first investigation of different N -body techniques was carried out over thirty years ago by Efstathiou et al. (1985). More recently, Heitmann et al. (2008) compared the halo abundance and the power spectrum of ten different N -body codes finding a ten percent spread between clustering properties of the codes. The measurement of the power spectrum with different mass assignment and aliasing correction schemes has also been subject to detailed investigation (Jing 2005; Cui et al. 2008; Colombi et al. 2009).

This paper studies some of the most important potential error sources of the simulation pipeline from the initial conditions to the power spectrum measurement at redshift zero. Potential errors are classified into four distinct categories: errors from the initial conditions, errors from the gravity calculation, and errors due to box-size and resolution effects. Each one of these categories is investigated separately with respect to the one percent convergence requirement.

The paper is structured as follows: section 2 summarises the characteristics of the used gravity codes and provides a convergence test between them. In section 3 and 4, we investigate the accuracy of initial conditions and study potential volume and resolution effects. Section 5 provides a list of requirements to obtain percent accuracy of the matter power spectrum and discusses consequences for simulating next-generation galaxy surveys.

2 COMPARING N -BODY CODES

The gravitational N -body technique is the standard tool to simulate the nonlinear Universe, yielding accurate results at scales where hydrodynamical effects are subdominant. Most N -body codes are either based on a particle-mesh method, a tree algorithm, or a hybrid combination of the two. In this paper, we compare the codes **Ramses**, **Pkdgrav3**, and **Gadget3**, which represent each of these three approaches and are widely used in the astrophysics and cosmology community.

The comparison is performed by running a simulation of box size $L = 500 h^{-1}\text{Mpc}$ and resolution of $N = 2048$ particles per dimension with each of the three codes, starting from the exact same initial conditions and using the standard run parameters described above. The initial conditions are based on second order Lagrangian perturbation theory (2LPT), generated at redshift 50 with a modified version of the IC code from Scoccimarro et al. (2012). For the cosmological parameters, we use Planck values, i.e., $\Omega_m = 0.3071$, $\Omega_\Lambda = 0.6929$, $\Omega_b = 0.0483$, $h = 0.6777$, $n_s = 0.9611$, and $\sigma_8 = 0.8288$ (Ade et al. 2014). The measurement of the

power spectra is performed at exactly the same redshifts and with the same analysis tool (using the triangular shaped cloud scheme for the mass assignment). In this way, we carefully avoid all other potential sources of error and directly compare effects due to the gravity calculations of the codes.

We now briefly present the three codes and give details about the run parameters for the comparison:

- The N -body and hydrodynamical code **Ramses** (Teyssier 2002) is based on a particle-mesh technique and uses adaptive mesh refinement for high density regions. The code is mainly used for hydrodynamical simulations in a cosmological context (Ocvirk et al. 2008; Agertz et al. 2010) but it has also been employed for pure dark matter N -body runs in the past (Teyssier et al. 2009; Rasera et al. 2014). For the comparison, we apply a coarse-level grid with refinement level $\ell_{\min} = 12$, corresponding to 2048^3 coarse cells. New refinements are triggered on a cell-by-cell, recursive basis when a cell collects more than 8 particles. Using this strategy we reach a maximum level of refinement $\ell_{\max} = 18$, corresponding to a spatial resolution of $2 h^{-1}\text{kpc}$. We employ adaptive, level-by-level time-stepping, with a time step size set smaller than the local free fall time, and by the requirement that a particle cannot move more than half a cell within one time step. The convergence criterion for the Poisson solver, defined as the ratio of the residual L^2 -norm to the right-hand side L^2 -norm, is set to $\epsilon = 10^{-4}$.

- The gravity code **Pkdgrav3** (an earlier version of which is described in Stadel 2001) is based on a binary tree algorithm using fifth order fast multipole expansion of the gravitational potential (using cell-cell interactions making it an $\mathcal{O}(N)$ gravity calculation method). Periodic boundary conditions are calculated with the Ewald summation technique, requiring very little data movement while exposing a high degree of parallelism. **Pkdgrav** has been extensively used for N -body simulations in the past, mainly in the context of cosmological zoom simulations such as *Via Lactea* (Diemand et al. 2007) and *Ghalo* (Stadel et al. 2009). The current version of **Pkdgrav** includes GPU acceleration for all force calculations, leading to a significant speed-up with respect to previous versions. In this paper, we use the run parameters $\epsilon = 0.02 l_{\text{mean}}$ (where l_{mean} is the mean particle separation) and $\theta = 0.7$ ($\theta = 0.55$ above redshift two) for softening and tree opening criteria. The adaptive time-stepping is parametrised in the standard way, i.e. $dt_i = \eta \sqrt{\epsilon/|a_i|}$ with $\eta = 0.15$ (where a_i is the acceleration of particle i). **Pkdgrav3** also has a more sophisticated time-stepping criterion based on an estimation of the local dynamical time.

- The tree-particle-mesh code **Gadget3** applies a uniform particle-mesh method at large scales plus a first order oct-tree technique at small scales (see Springel 2005, for a description of an earlier version of the code). **Gadget** is extensively used in many contexts and is most known for the *Millennium* suite of cosmological simulations (Springel et al. 2005), as well as the *Aquarius* zoom simulations (Springel et al. 2008). For the comparison, we use a comoving Plummer-equivalent softening length of $\epsilon = 10 h^{-1}\text{kpc}$ and the code's relative tree opening criterion with a tolerance value of $\alpha = 0.005$ for the gravitational force accuracy (see Springel 2005, for more information). Furthermore, we adopt a time integration parameter corresponding to $\eta = 0.22$ for the time-

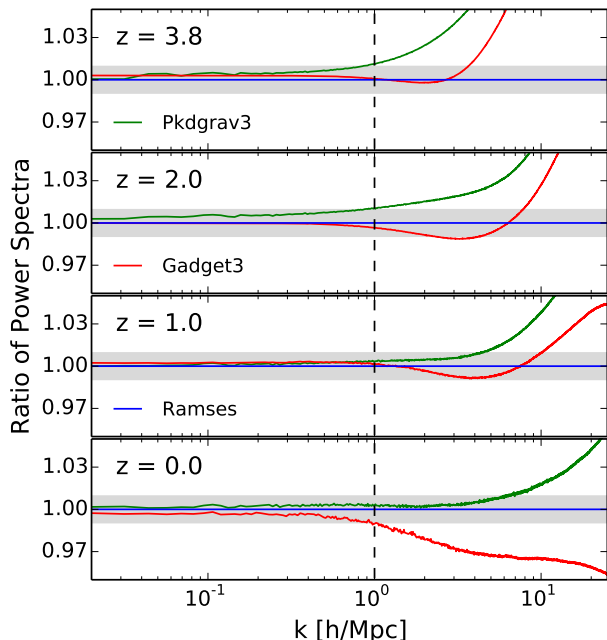


Figure 1. Comparison of Power Spectra from the three different N -body codes at different redshifts. Green lines correspond to `Pkdgrav3`, red lines to `Gadget3`, and blue lines to `Ramses` (reference lines). One percent agreement (indicated by the grey band) is obtained for $k \leq 1 \text{ h Mpc}^{-1}$ (dashed vertical line).

stepping criterion used above in `Pkdgrav3`. The long-range particle-mesh forces are calculated with a 2048^3 Fourier grid.

All simulations of the comparison were performed on the hybrid CPU/GPU cluster *Piz Daint* at the Swiss National Supercomputing Centre (CSCS). The total run-time for the three codes is 94352 node-hours for `Ramses`, 34524 node-hours for `Gadget3`, and 1632 node-hours for `Pkdgrav3` (the former two codes were run on 512 nodes using CPU only, while the latter was run on 128 nodes using full GPU acceleration for the force calculations). On each node of *Piz Daint* there are 8 CPU-cores and one Nvidia Tesla K20X GPU accelerator.

The resulting power spectra of the code comparison are shown in Fig. 1, where different panels correspond to different redshifts $z = 3.8, 2, 1.0$, and 0.0 . The green lines refer to `Pkdgrav3`, the red lines to `Gadget3`, and the blue lines to `Ramses`⁴. One percent agreement (grey shaded area) between the different codes is obtained up to $k \sim 1 \text{ h Mpc}^{-1}$ over all redshifts, as illustrated by the vertical dashed line. In the highly nonlinear regime from $k = 1$ to 10 h Mpc^{-1} , the agreement between codes is at the three percent level for $z = 1$ and below⁵. At higher redshifts, the discrepancy grows, reaching about five percent at $z = 2$ and ten percent at $z = 3.8$.

The agreement between the codes is significantly better

⁴ We have chosen the blue lines to act as reference, solely because it lies between the green and red lines at $z = 0$, therefore improving the readability of the plots.

⁵ While `Ramses` and `Pkdgrav3` show percent agreement until $k \sim 7 \text{ h Mpc}^{-1}$, `Gadget` slightly deviates at $k \sim 1 \text{ h Mpc}^{-1}$.

than in the previous code comparison project by Heitmann et al. (2008, hereafter H08) illustrating the progress in code development over the last decade. For example, at very large scales `Pkdgrav` and `Gadget` now agree within ~ 0.3 percent compared to ~ 1.2 percent in H08. Furthermore, the prominent systematic offset between PM-codes and tree-codes visible in H08 (with more than 10 percent difference at $k \sim 10 \text{ h Mpc}^{-1}$) has now entirely disappeared.

The results of the code comparison are based on the standard run parameters described above. These parameters have never been systematically tested in the context of large-scale cosmological simulations, but they emerged via many different code applications in the past. However, finding more optimal code parameters is non-trivial because the true power spectrum is not known *a priori*. Parameters cannot simply be tuned to achieve maximal agreement between codes since this could lead to convergence towards the wrong answer.

It is nevertheless important to quantify the dependency of the run parameters on the resulting power spectrum. Only results which are insensitive to the choice of code parameters can be trusted. In the Appendix we study the effects of the most sensitive code parameters, which are the size of the PM grid for `Gadget3` as well as the time-stepping criterion for all three codes. We conclude that reasonable variations of these parameters lead to sub-percent effects on the power spectrum below $k \sim 10 \text{ h Mpc}^{-1}$, smaller than the observed differences between codes visible in Fig. 1.

Summing up, the code comparison suggests that the consensus between different N -body techniques is good, however not quite good enough for the targeted percent accuracy up to $k \sim 10 \text{ h Mpc}^{-1}$. Further improvements to the codes will not be easily achievable as the correct solution for the matter power spectrum is not known. A common effort of the community is required to converge towards a generally accepted solution. In order to encourage further comparison of N -body codes, we release the IC file used here plus all power spectrum measurements on www.ics.uzh.ch/~aurel/.

3 INITIAL CONDITIONS

Initial conditions of cosmological simulations are generated as a random realisation of a (Gaussian) density field, based on either first or second order Lagrangian perturbation theory. The density field is usually discretised in form of aligned particles on an initial grid, where small displacements account for the initial perturbations.

The redshift of the initial conditions has to be chosen with care. It should lie in a range where all resolved perturbations are large enough to dominate numerical noise, but still small enough to be accurately described by perturbation theory. It has been shown in the past that it is advantageous to use second order Lagrangian perturbation theory (2LPT) with respect to the simpler first order or Zel'dovich approximation (ZA), as it allows for smaller starting redshifts, further away from the noise dominated high-redshift regime (Crocco et al. 2006; Jenkins 2010; Reed et al. 2013).

We study the effects of the initial conditions on the power spectrum at redshift zero by running simulations with $L = 512 \text{ h}^{-1} \text{ Mpc}$ and $N = 1024$ particles per dimension

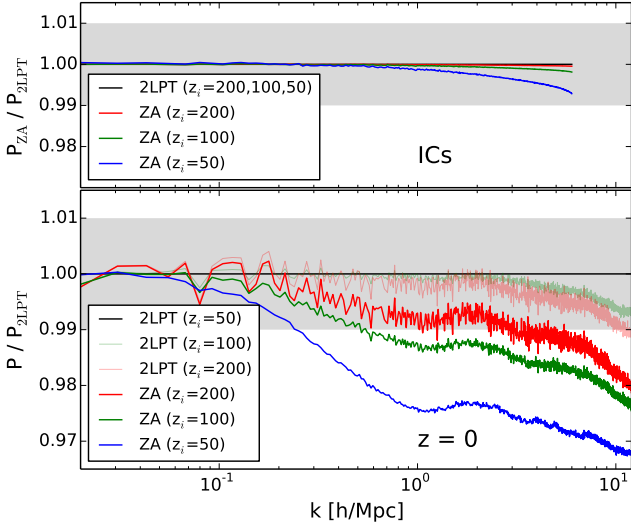


Figure 2. Comparison between power spectra from simulations with ZA and 2LPT initial conditions. Top panel: Ratios of ZA versus 2LPT at $z_i = 50$ (blue), $z_i = 100$ (green), and $z_i = 200$ (red) directly measured from the ICs. Bottom panel: Ratios of various ZA and 2LPT runs with respect to the 2LPT ($z_i = 50$) reference line (black) at redshift zero. Bold lines refer to ZA with $z_i = 50$ (blue), $z_i = 100$ (green), and $z_i = 200$ (red), faint lines refer to 2LPT with $z_i = 100$ (green) and $z_i = 200$ (red). One percent agreement is illustrated by the grey band.

with the N -body code `Pkdgrav`. The initial conditions are generated with `MUSIC` (Hahn & Abel 2011), using both the ZA and 2LPT approach at different starting redshifts.

The resulting effects on the power spectrum are illustrated in Fig. 2. In the top panel, we show the ratios between ZA and 2LPT directly measured in the ICs at the corresponding starting redshifts of $z_i = 200$ (red line), $z_i = 100$ (green line), and $z_i = 50$ (blue line). The differences between ZA and 2LPT are at sub-percent level (converging towards high redshifts) and limited to high wave numbers above $k \sim 1 \text{ h Mpc}^{-1}$. In the bottom panel, we illustrate the situation at redshift zero, now taking the 2LPT-run with $z_i = 50$ as reference (black line). For the ZA-simulation with $z_i = 50$, the deviation has grown substantially with respect to the ICs and is visible down to $k \sim 0.1 \text{ h Mpc}^{-1}$. This somewhat surprising behaviour is in agreement with previous findings (Knebe et al. 2009; Heitmann et al. 2010; L’Huillier et al. 2014). The ZA-runs with higher starting redshifts of $z_i = 100$ (green line) and $z_i = 200$ (red line) slowly converge towards the black reference line but do not reach percent agreement. Unlike the ZA, simulations with 2LPT are converged within one percent between all starting redshifts investigated here. This is illustrated by the faint green and red lines representing the 2LPT-runs with $z_i = 100$ and $z_i = 200$.

Fig. 2 suggests that a starting redshift $z_i > 200$ is required to obtain percent accuracy with ZA initial conditions. Such high starting redshifts are prone to numerical problems, since N -body codes do not deal well with extremely small initial density perturbations. At what redshift numerical effects become a problem depends on the code and the run parameters. Based on a study involving `Pkdgrav2` and `Gadget2`, Reed et al. (2013) concluded that the initial red-

shift and the redshift of typical halo formation should not differ by more than a factor of fifty. For the cosmological boxes investigated here, most haloes form around redshift two (see for example McBride et al. 2009) and the initial redshift should therefore not exceed $z = 100$.

In agreement with previous results, we conclude that initial conditions with 2LPT should be used consistently for cosmological simulations. They are significantly more accurate than ZA initial conditions and they allow lower starting redshifts, thus decreasing the run-time of simulations.

4 BOX SIZE AND RESOLUTION

A careful setup of simulations in terms of box size and particle numbers is crucial in order to obtain one percent agreement in the power spectrum. Small boxes tend to suffer from sampling variance and missing large-scale modes, while large boxes might not have enough resolution to capture the very nonlinear scales.

We use `Pkdgrav3` to run a suite of numerical simulations with varying box size and particle number. Volume effects on the power spectrum are investigated by comparing simulations with the same mass resolution and different box sizes. Effects due to particle numbers are studied with runs of constant box sizes. All simulations are based on 2LPT initial conditions, generated with `MUSIC` at redshift 50.

The power spectrum is measured with triangular shaped cloud (TSC) mass assignment on a 8192^3 grid. For all measurements, we subtract the Poisson shot-noise contribution due to the simulation particles, given by $P_{\text{sn}} = (L/N)^3$. The statistical error on the power spectrum consists of a sample variance and a shot-noise contribution and is given by $\sigma_P = (2/\Delta N_m)^{1/2}(P + P_{\text{sn}})$, where $\Delta N_m = L^3 k^2 \Delta k / (2\pi^2)$ is the number of modes per k -bin.

In the left panel of Fig. 3, we illustrate ratios of power spectra from runs with the same mass resolution but different box sizes and particle numbers. The particle mass is kept constant at $M_p \sim 10^{10} h^{-1} M_\odot$, while the box length is increased together with the number of particles. A small box with $L = 128 h^{-1} \text{Mpc}$ (blue line) underestimates the power by more than 10 percent. Doubling the box size to $L = 256 h^{-1} \text{Mpc}$ (green line) leads to an overall accuracy of 5 percent (one percent at small scales, $k > 1 \text{ h Mpc}^{-1}$). Boxes with length of $L = 512 h^{-1} \text{Mpc}$ (red line) and more ($L = 1024 h^{-1} \text{Mpc}$, black reference line) differ by less than one percent over the entire range of wave numbers. We therefore conclude that the box size of simulations should not be smaller than $500 h^{-1} \text{Mpc}$ in order to eliminate all *nonlinear* finite-volume effects at the required percent precision. This is not the same than standard Gaussian sample variance which requires an even larger minimal box size of $L \sim 2 h^{-1} \text{Gpc}$ (Mohammed & Seljak 2014).

In the right panel of Fig. 3, we plot power spectra from runs with the same box size ($L = 512 h^{-1} \text{Mpc}$) and different particle numbers, effectively increasing the mass resolution. Simulations with $N = 256$ (blue line), $N = 512$ (green line), and $N = 1024$ (red line) underestimate the power on small scales with respect to the $N = 2048$ reference run (black line). The divergence from percent accuracy happens roughly at the scale where shot-noise from the simulation particles becomes relevant (the wave number where

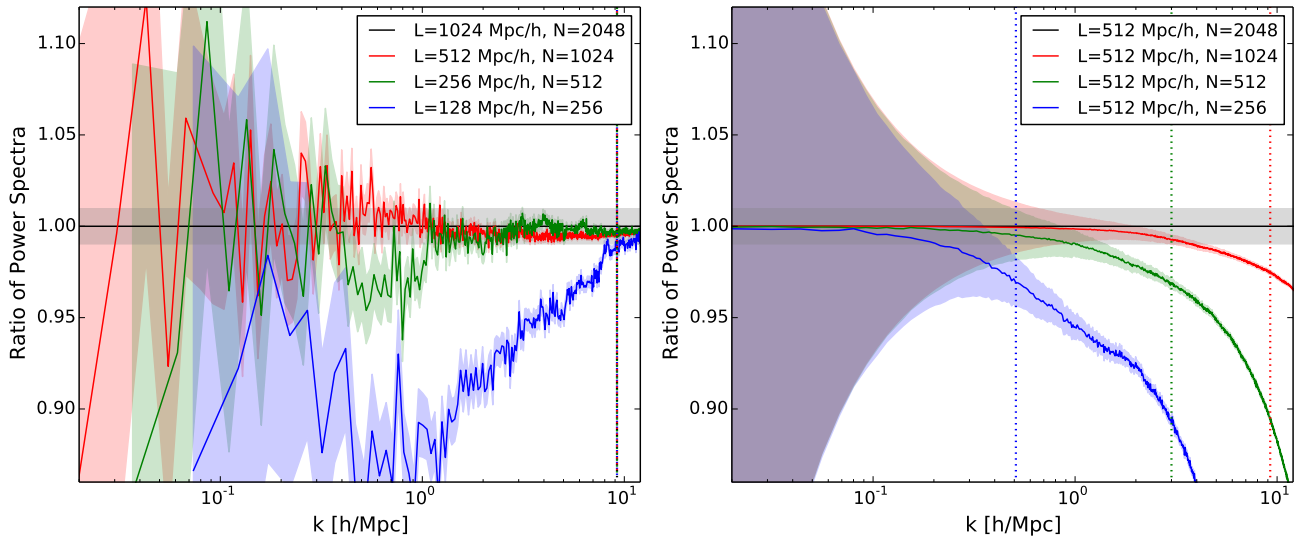


Figure 3. Investigating box size and resolution effects on the power spectrum. Left panel: Same physical resolution and increasing box size: $L=128 h^{-1}\text{Mpc}$ (blue), $L=256 h^{-1}\text{Mpc}$ (green), $L=512 h^{-1}\text{Mpc}$ (red), $L=1024 h^{-1}\text{Mpc}$ (black, reference line). Right panel: Same box size ($L=512 h^{-1}\text{Mpc}$) and increasing number of particles (per dimension): $N=256$ (blue), $N=512$ (green), $N=1024$ (red), and $N=2048$ (black, reference line). The coloured areas quantify the statistical errors from sample variance and shot noise, while the grey shaded band highlights the range of percent accuracy. Dotted vertical lines indicate where the shot-noise contribution exceeds one percent.

the shot-noise contribution to the measured power spectrum reaches one percent is indicated with colour-dotted vertical lines).

The drop in power of the lower resolution runs, visible in the right panel of Fig. 3, can be explained in terms of analytical considerations: experiments with the halo model show that clusters significantly contribute to the power spectrum, while the presence of small haloes below $10^{11} h^{-1}\text{M}_{\odot}$ have a negligible effect (Schneider et al. 2012; van Daalen & Schaye 2015). Since the simulations with lower resolution (represented by the coloured dots) do not resolve haloes down to masses of $10^{11} h^{-1}\text{M}_{\odot}$, they underestimate the physical power at small scales. The $N = 2048$ simulation on the other hand, has a particle mass of $M_p \sim 10^9 h^{-1}\text{M}_{\odot}$, resolving $10^{11} h^{-1}\text{M}_{\odot}$ haloes with ~ 100 particles. Moreover, the convergence rate in the plot suggests that the $N = 2048$ run is one percent accurate until $k \sim 10 h \text{Mpc}^{-1}$.

Based on the right-hand-side panel of Fig. 3, we can determine a minimal mass resolution required to obtain percent convergence in the matter power spectrum. Since the runs illustrated by the blue, green, and red lines underestimate the power by more than a percent for values above $k = 0.25, 1, 4 h \text{Mpc}^{-1}$, we can safely expect the black line to depart from the true answer beyond $k = 10 h \text{Mpc}^{-1}$. A conservative estimate therefore yields a maximum simulation particle mass of $M_p = 10^9 h^{-1}\text{M}_{\odot}$ guaranteeing a percent converged power spectrum at all scales up to $k = 10 h \text{Mpc}^{-1}$. This requirement can be relaxed to $M_p \sim 8 \times 10^{10} h^{-1}\text{M}_{\odot}$ for wave numbers up to $k = 1 h \text{Mpc}^{-1}$ (as shown by the green line). Numerical simulations for upcoming survey missions need large boxes of at least $4 h^{-1}\text{Gpc}$ to cover the entire survey volume (Ivezic et al. 2008; ?). This means that at least $N = 16000$ particles per dimension (i.e four

trillion in total) are required to reach percent precision for the power spectrum up to $k \sim 10 h \text{Mpc}^{-1}$.

After investigating the convergence with respect to box size and mass resolution, we present a suite of four simulations with each $N = 2048$ per dimension and decreasing box sizes of $L = 4096, 2048, 1024,$ and $512 h^{-1}\text{Mpc}$. These simulations provide a combined measurement of the power spectrum over the entire range of scales from $k \sim 0.05 h \text{Mpc}^{-1}$ to $k \sim 10 h \text{Mpc}^{-1}$.

In Fig. 4 we use the combined power spectrum from these four simulations as reference line, where the different colours indicate which simulation as been used for which k -range. The colour-shaded areas furthermore indicate the uncertainties due to sample variance and the grey-shaded area delimits the range of percent precision. In Fig. 4 the Franken emulator (Heitmann et al. 2008, solid black line), the halofit model (Takahashi et al. 2012, dashed black line), and the linear theory (dotted black line) are plotted against the reference line from our simulations. The halofit model is a revised version of the Smith et al. (2003) fitting scheme (Takahashi et al. 2012), which is physically motivated by the halo model and claims to be 10 percent accurate for $k \leq 1 h \text{Mpc}^{-1}$ between $z = 0$ and $z = 10$. Compared to our simulations the agreement is better than 5 percent over all measured scales and redshifts. The cosmic Franken emulator is an interpolation tool based on a suite of simulations with varying cosmological parameters (Heitmann et al. 2010, 2014). The agreement between the emulator and our simulations is about three percent at $z = 0$ and five percent at $z = 1$. This is roughly within the stated accuracy of Heitmann et al. (2014). However, our simulations consistently predict more power than the cosmic emulator at scales around $k \sim 1 h \text{Mpc}^{-1}$ and above, confirming results from Skillman et al. (2014) who observe a similar departure

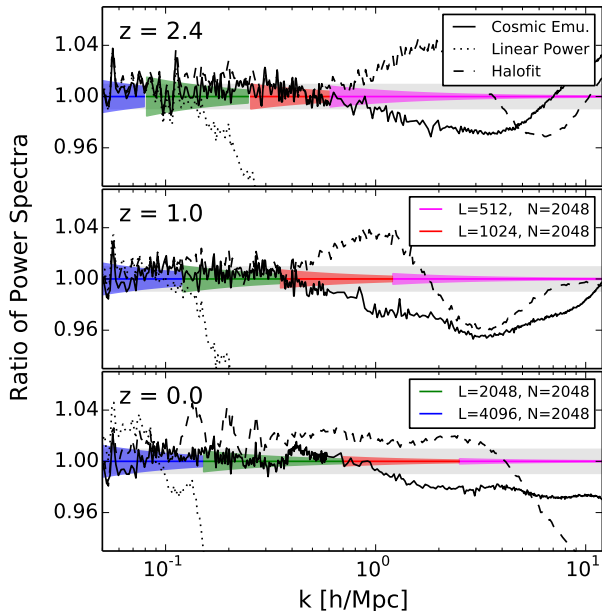


Figure 4. Power spectra of the cosmic Franken emulator (Heitmann et al. 2014), the revised halofit function (Takahashi et al. 2012), and the linear prediction compared to the outcome of simulations with $N = 2048$ particles per dimension and varying box size $L = 512 h^{-1}\text{Mpc}$ (magenta), $L = 1024 h^{-1}\text{Mpc}$ (red), $L = 2048 h^{-1}\text{Mpc}$ (green), $L = 4096 h^{-1}\text{Mpc}$ (blue). Coloured areas quantify the statistical errors from sample variance and shot-noise, the grey shaded band highlights the range of percent accuracy.

from the cosmic emulator. Part of the difference should come from the fact that the emulator was calibrated with **Gadget** runs, while we use **Pkdgrav**, two codes that differ by about three percent at $k > 1 h \text{Mpc}^{-1}$ as illustrated in Fig. 1.

5 CONCLUSIONS

The future of cosmology relies on data from large scale structure surveys. This data can only be fully exploited if we understand gravitational clustering and galaxy formation at high accuracy. The matter power spectrum, as the prime statistical measure, needs to be known within percent precision from linear scales up to $k \sim 10 h \text{Mpc}^{-1}$.

Although cosmological N -body techniques have been developed and constantly improved during the last two decades, obtaining the required accuracy remains a challenge. The entire pipeline from the generation of initial conditions to the analysis of the final data needs to be examined carefully and potential sources of error have to be quantified.

In this paper, we compare power spectra of simulations from the three gravity codes **Ramses**, **Pkdgrav3**, and **Gadget3**. These codes are well established in the community and represent common N -body techniques for cosmological simulations: the particle-mesh technique, the tree method, and a hybrid combination of the two. In a second part, we explore potential error sources from *initial conditions*, *simulation volume*, and *resolution*, investigating effects on the matter power spectrum. These findings are then expressed in terms of a minimal volume and minimal mass resolution requirement to obtain the targeted percent accuracy.

The main results of the paper can be summarised as follows:

(i) *Gravity calculation:* The gravity codes **Ramses**, **Pkdgrav3**, and **Gadget3** agree within one percent up to $k = 1 h \text{Mpc}^{-1}$ (over all studied redshifts), and within three percent up to $k = 10 h \text{Mpc}^{-1}$ (below redshift one).

(ii) *Simulation volume:* A minimum box size of $L \sim 0.5 h^{-1}\text{Gpc}$ is needed to avoid nonlinear finite-volume effects at the percent level of the power spectrum. Reducing sample variance below one percent requires an even larger box size of $L \sim 2 h^{-1}\text{Gpc}$.

(iii) *Mass resolution:* A conservative estimate of the maximum particle mass in simulations yields $M_p = 10^9 h^{-1}M_\odot$ for percent accurate power spectra up to $k = 10 h \text{Mpc}^{-1}$. This requirement can be relaxed to $M_p \sim 8 \times 10^{10} h^{-1}M_\odot$, if only wave numbers up to $k = 1 h \text{Mpc}^{-1}$ are considered. Upcoming surveys, such as **DES**, **LSST**, and **Euclid**, require large simulation volumes of $L \sim 4 h^{-1}\text{Gpc}$ or more. As a consequence, numerical simulations need to have at least $N \sim 16000$ particles per dimension (i.e four trillion in total) to reproduce the power spectrum at targeted accuracy.

(iv) *Initial conditions:* Initial conditions based on the Zel’dovich approximation (ZA) require very high starting redshifts of $z = 200$ or above. Such high redshifts are prone to numerical errors, since the size of perturbations are of the order of the numerical accuracy. Initial conditions based on second order Lagrangian perturbation theory (2LPT) are significantly more accurate. They allow late starting redshifts, reducing the run-time of simulations and minimising potential numerical errors in the high redshift regime.

Summarising these results, it is possible to run cosmological simulations with sub-percent errors from volume and mass resolution effects, however, at the price of very high particle numbers. In terms of the gravity calculation, the agreement between codes is good, but not quite at the percent level for the very nonlinear regime.

In the future, it will be crucial to include baryonic effects driven by AGN feedback, as they have been shown to significantly affect the matter power spectrum at nonlinear scales (van Daalen et al. 2011; Angulo et al. 2013). Quantifying and parametrising the AGN feedback will be one of the main challenges of computational cosmology, and a basic requirement to take full advantage of the upcoming large scale structure observations.

DATA RELEASE

All relevant data of the code comparison project, i.e. the IC file, run parameters, and power spectra measurements, can be found at www.ics.uzh.ch/~aure1/. We hope that this information will be useful for future comparison and accuracy tests including other N -body codes.

ACKNOWLEDGEMENTS

This work was initiated within the framework of the Cosmological Simulation Working Group of the Euclid Consortium. AS is supported by the Synergia project “Euclid” from the Swiss National Science Foundation. VS acknowledges

support from the Deutsche Forschungsgemeinschaft (DFG) through Transregio 33, “The Dark Universe”. All simulations were run on the *Piz Daint* cluster at the Swiss National Supercomputer Centre (CSCS) under the project allocation s511.

REFERENCES

- Ade, P. A. R., et al. 2014, *A&A*, 571A, 16P
 Agertz, O., Teyssier, R., Moore, B. 2011, *MNRAS*, 410, 1391A
 Angulo, R. E., Hahn, O., Abel, T. 2013, *MNRAS*, 434, 1756A
 Cui, W. Liu, L. Yang, X. Wang Y. Feng, L. Springel, V. 2008, *ApJ*, 687, 738C
 Colombi, S., Jaffe, A., Novikov, D., Pichon, C. 2009, *MNRAS*, 393, 511
 Crocce, M., Pueblas, S., Scoccimarro, R. 2006, *MNRAS*, 373, 369C
 Diemand, J., Kuhlen, M., Madau, P. 2007, *ApJ*, 657, 262D
 Efsthathiou, G., Davis, M., White, S. D. M., Frenk, C. S. 1985, *ApJS*, 57, 241E
 Fosalba, P., Crocce, M., Gaztañaga, E., Castander, F. J. 2015, *MNRAS*, 448, 2987F
 Hahn, O., Abel, T. 2011, *MNRAS*, 415, 2101H
 Heitmann, K. et al. 2008, *CS&D*, 1a5003H
 Heitmann, K., White, M., Wagner, C., Habib, S., Higdon, D. 2010, *ApJ*, 715, 104H
 Heitmann, K., Lawrence, E., Kwan, J., Habib, S., Higdon, D. 2014, *ApJ*, 780, 111H
 Ivezić, Z. et al. 2008, arXiv:0805.2366
 Jenkins, A. 2010, *MNRAS*, 403, 1859J
 Jing, Y. P. 2005, *ApJ*, 620, 559J
 Carlson, J., White, M., Padmanabhan, N. 2009, *PRD*, 80, 043531
 Knebe, A., Wagner, C., Knollmann, S., Diekershoff, T., Krause, F. 2009, *ApJ*, 698, 266K
 L’Huillier, B., Park, C., Kim, J. 2014, *NewAst.* 30, 79L
 McBride, J., Fakhouri, O., Ma, C.-P. 2009, *MNRAS*, 398, 1858M
 Mohammed, I. & Seljak, U. 2014, *MNRAS*, 445, 3382M
 Mohammed, I., Martizzi, D., Teyssier, R., Amara, A. 2014, arXiv:1410.6826
 Ocvirk, P., Pichon, C., Teyssier, R. 2008, *MNRAS*, 390, 1326O
 Rasera, Y., Corasaniti, P.-S., Alimi, J.-M., Bouillot, V., Reverdy, V., Balms, I. 2014, *MNRAS*, 440, 1420R
 Reed, D. S., Smith, R. E., Potter, D., Schneider, A., Stadel, J., Moore, B. 2013, *MNRAS*, 431, 1866R
 Schneider, A., Smith, R. E., Macciò, A. V. Moore, B. 2012, *MNRAS*, 424, 684S
 Scoccimarro, R., Hui, L., Manera, M., Chan, K. C., *PRD*, 85, 083002
 Skillman, S. W., Warren, M. S., Turk, M. J., Wechsler, R. H., Holz, D. E., Sutter, P. M. 2014, arXiv:1407.2600
 Smith, R. E., Reed, D. S., Potter, D., Marian, L., Crocce, M., Moore, B., 2014, *MNRAS*, 440, 249S
 Smith, R. E., Peacock, J. A., Jenkins, A., White, S. D. M., Frenk, C. S., Pearce, F. R., Thomas, P. A., Efsthathiou, G., Couchman, H. M. P., 2003, *MNRAS*, 341, 1311S
 Springel, V. 2005, *MNRAS*, 364, 1105S
 Springel, V. et al., 2005, *Nature*, 435, 629S
 Springel, V., Wang, J., Vogelsberger, M., Ludlow, A., Jenkins, A., Helmi, A., Navarro, J. F., Frenk, C. S., White, S. D. M. 2008, *MNRAS*, 391, 1685S
 Stadel, J. G. 2001, Thesis (PhD), University of Washington.
 Stadel, J., Potter, D., Moore, B., Diemand, J., Madau, P., Zemp, M., Kuhlen, M., Quilis, V. 2009, *MNRAS*, 398L, 21S
 Takahashi, R., Sato, M., Nishimichi, T., Taruya, A., Oguri, M. 2012, *ApJ*, 761, 152T
 Teyssier, R., 2002, *A&A*, 385, 337T
 Teyssier, R., Pires, S., Prunet, S., Aubert, D., Pichon, C., Amara, A., Benabed, K., Colombi, S., Refregier, A., Starck, J.-L. 2009, *A&A*, 497, 335T
 van Daalen, M. P., Schaye, J., Booth, C. M., Dalla Vecchia, C. 2011, *MNRAS*, 415, 3649V
 van Daalen, M. P., Schaye, J. 2015, arXiv:1501.05950

APPENDIX A: VARIATION OF CODE PARAMETERS

In the main text, we use standard code parameters from the literature to compare the different gravity codes. This is justified because the exact solution of the power spectrum is not known at nonlinear scales, and a posterior adjustment of code parameters would lead to a false impression of convergence. It is nevertheless important to quantify how the choice of code parameters affects the final results.

In general, code accuracy parameters can either be attributed to the force calculation or the time-stepping. Typical parameters regulating the force accuracy are softening-length and opening-angle for tree-codes (such as `Pkdgrav3`) as well as grid refinement strategy and accuracy of the Poisson solver for adaptive PM codes (such as `Ramses`). Hybrid codes (such as `Gadget3`) usually have an additional parameter regulating the transition scale between the PM and tree regime. The accuracy of time integration, on the other hand, is usually controlled by the adaptive time-stepping criterion which is implemented in a similar way in all three codes.

Past work has shown that for tree codes softening and tree-opening criteria show percent convergence at $k \leq 10 h \text{Mpc}^{-1}$ for reasonable parameter choices (Reed et al. 2013; Smith et al. 2014). The same seems true for the force accuracy parameters of adaptive PM codes which have shown to yield the same precision than generic tree-codes (Teyssier 2002). More significant deviations are reported for the transition parameter between the PM and tree regimes in hybrid codes (Smith et al. 2014) and for the time-stepping criterion affecting all three codes (Reed et al. 2013). In the following, we investigate the effects of both time-stepping and PM-grid transition on the resulting power spectrum.

In order to test the effect of time-stepping, we run simulations with alternative time-stepping criteria for all three codes of the comparison project. For `Ramses` and `Gadget3` we use the global time-stepping mode as an alternative, where *all* particles trajectories are integrated with the smallest time-stepping of the adaptive (default) mode independently of their gravitational acceleration. For `Pkdgrav` we keep the adaptive nature of time-stepping and vary the time-stepping parameter η around the default choice $\eta = 0.15$.

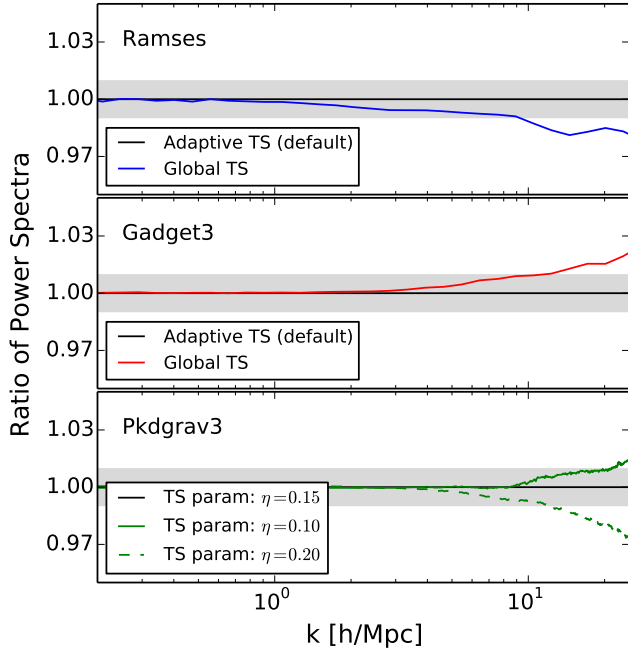


Figure A1. Effects of different time-stepping strategies on the power spectrum. Top: Adaptive (default) versus global time-stepping for **Ramses**. Centre: Adaptive (default) versus global time-stepping for **Gadget3**. Bottom: Different values for the time-stepping parameter η around the default value $\eta = 0.15$ for **Pkdgrav3**.

The impact of the time-stepping on the power spectrum is illustrated in Fig. A1. Switching to global time-stepping affects the result at the percent level around $k \sim 10 \text{ h Mpc}^{-1}$ for both **Ramses** and **Gadget3**, however, with an inverse general trend (reducing power for **Ramses** and increasing it for **Gadget3**). Varying the η parameter in **Pkdgrav3** around $\eta = 0.1 - 0.2$ also leads to a percent effect on the power spectrum at $k \sim 10 \text{ h Mpc}^{-1}$ (bottom panel), with the general trend of increasing power for smaller time-steps. Based on these tests we conclude that the results from the code comparison (i.e., Fig. 1) are not sensitive to the time-step criterion as long as *reasonable* parameter choices are considered.

The effect of the PM-grid transition in **Gadget** is investigated by running simulations with different size of the PM grid around the default choice (where the number of grid points equals the particle number, i.e., PM-grid = N). The resulting power spectra are illustrated in Fig. A2, showing differences at the percent level over various scales. The size of the scatter seems significant for precision cosmology and requires further investigation. However, the variation is not large enough to explain the offset between **Gadget** and **Ramses**/**Pkdgrav3** in the $z = 0$ panel of Fig. 1.

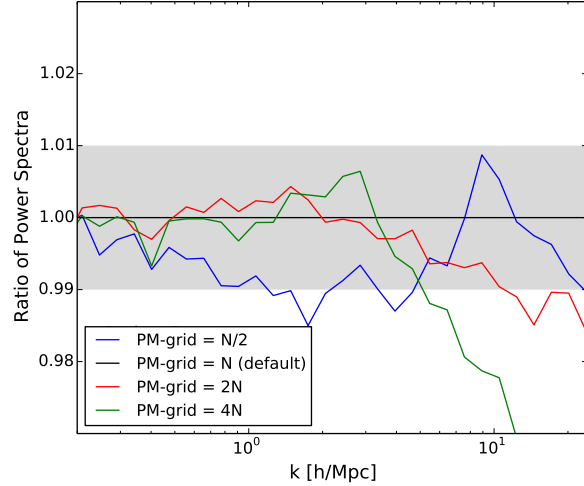


Figure A2. Effects of different sizes of the PM-grid on the power spectrum.